UNIVERSITY OF LEEDS

This is a repository copy of *Substituents modulate biphenyl penetration into lipid membranes*.

Article:

eprints@whiterose.ac.uk
https://eprints.whiterose.ac.uk/

Accepted Manuscript

Substituents modulate biphenyl penetration into lipid membranes

A. Rashid, A. Vakurov, S. Mohamadi, D. Sanver, A. Nelson

Substituents modulate biphenyl penetration into lipid membranes

A. Rashid[a], A.Vakurov, S.Mohamadi, D.Sanver and A.Nelson*

School of Chemistry, University of Leeds, Woodhouse lane, Leeds, LS2 9JT,UK.

[a]present address, University of Engineering and Technology, Lahore, Pakistan.

*corresponding author, a.l.nelson@leeds.ac.uk

Abstract

Electrochemical impedance techniques and fluorescence spectroscopic methods have been applied to the study of the interaction of ortho (o)-, meta (m)- and para (p)-Cl-, o-, m- and p-HO-, p-H_3CO-, p-H_3C-, p-NC- and p-O_3^-S- substituted biphenyls (BPs) with Hg supported dioleoyl phosphatidylcholine (DOPC) monolayers and DOPC vesicles. Non-planar o-substituted BPs exhibit the weakest interactions whereas planar p-substituted BPs interact to the greatest extent with the DOPC layers. The substituted BP/DOPC monolayer and bilayer interaction depends on the effect of the substituent on the aromatic electron density, which is related to the substituents' mesomeric Hammetts constants. Substituted BPs with increased ring electron density do not increase the DOPC monolayer thickness on Hg and penetrate the DOPC vesicle membranes to the greatest extent. Substituted BPs with lower ring electron density can cause an increase in the monolayer's thickness on Hg depending on their location and they remain in the interfacial and superficial layer of the free standing DOPC membranes. Quantum mechanical calculations correlate the binding energy between the substituted BP rings and methyl acetate, as a model for the $-CH_2-(CO)O-CH_2-$ fragment of a DOPC molecule, with the location of BPs within the DOPC monolayer.

Keywords: Electrochemical impedance, Fluorescence quenching, Phospholipid monolayers/bilayers, Monosubstituted biphenyls, Hammetts constants.

1. Introduction

Biphenyl (BP) and its derivatives are well known for their thermal stability, electrical insulation and resistance to redox processes and have been widely used in the past in transformers and capacitors as dielectric fluids [1,2]. Moreover, these substance have also been employed in the preparation of pesticides, optical brighteners [3], and as fungicides in waxing many fruits. However substituted BPs are established environmental toxins [4]. Chlorobiphenyls (Cl-BPs) have been a significant issue for their toxicity, bioaccumulation and environmental persistence because of their stability [5]. BPs and Cl-BPs are metabolised to hydroxy biphenyls (HO-BPs) via formation of the arene oxide intermediate [6] with para (p)-hydroxybiphenyl (p-HO-BP) as a major product [5,7,8]. In addition to the monohydroxy metabolites, dihydroxy products can also be produced as a result of hydroxylation of BP. The hydroxy metabolites of Cl-BPs have been shown to be retained in the blood of many animals and humans [9-12]. The structures of these metabolites resemble thyroid hormones in possessing two aromatic rings and are reported as endocrine disrupters because they compete with thyroxin for its active site [13,14].

In ortho (o-) substituted BPs, the two phenyl rings have been reported to exhibit a twisted conformation with an increase in the torsional angle ($\prod$) between the phenyl rings from 42.5˚ to 63.2˚ depending on the size of the substituent (Br>Cl>F). This can be explained by the destabilization effect based on the hydrogen substituent repulsion in the o- position. Changes in the molecular structure caused by substitution at the p- position does not affect the structure of BP derivatives compared to the unsubstituted BP in both ground and excited states [15]. The value of $\prod$ for m- and p- substituted BPs is around 42-45˚ but for o-substituted BPs, $\prod$ is around 63˚. m-substituted BPs have a higher barrier height for rotation between 0˚-90˚ than p- substituted BPs which is responsible for slightly higher values of $\prod$ [16]. Hence coplanarity of the two phenyl rings

decreases in the following order depending on the position of substitution: BP ≈ p-substituted BP > m-substituted BP > o-substituted BP. There have been many studies on the potential toxicity of substituted BPs in vivo [2,17,18] but very little work has been carried out on the evaluation of the molecular characteristics responsible for their toxicity and the mechanism of their interaction at a cellular and plasma membrane level. According to some studies, non-planar o-substituted BPs increased the cell membrane leakiness and decreased the membrane integrity compared to the planar BPs [17-19]. While other studies have shown the non-planar o-substituted molecules to be less active compared to the planar p-substituted molecules because of the steric hindrance of the o-substituted species which influences their penetration into the phospholipid membrane [20-22]. Indeed reference [22] used electrochemical methods in a preliminary study of the relation between the biphenyl's structure and their interaction with lipid layers however no understanding was developed concerning a systematic structure-activity relationship.

The present study is an attempt to widen and deepen the work begun in reference [22] by extending the electrochemical methods and supporting them with additional techniques. An important objective of this work was to obtain an understanding of the fundamental molecular properties of aromatic and associated molecular species which enhance their interaction with phospholipid membranes as a model for biological membranes. Of interest in particular was how the substituted biphenyl affected the membrane structure, function and biomolecular organization and how this related to membrane surface interactions with the biphenyl. The final location of the substituted biphenyl in the membrane following interaction was also sought. An understanding of the factors promoting aromatic group interaction with phospholipid membranes is extremely relevant to biological membrane structure and function. A significant reason for this is that the conformation of membrane proteins and peptides is strongly affected by their aromatic residue interaction with the phospholipid skeleton [23-25].

3

Hg supported phospholipid monolayers and free standing bilayer vesicles have been used to investigate: (1) structure-activity relationships and (2) mechanism of interaction of BP derivatives, with phospholipid layers, using electrochemical and fluorescence spectroscopic techniques. The rationale for employing these techniques was to obtain a generic and consistent understanding of the interaction mechanism. DOPC was used as the test phospholipid in these studies. The model system of DOPC monolayer on Hg is a well established membrane model which has been well characterized internationally [26-35]. Moreover it has been shown to be particularly stable and reproducible in structure. Although Hg supports monolayers of palmitoyloleoyl PC (POPC) and POPC/POPE mixtures, it was felt appropriate to carry out this study with DOPC on Hg in the first instance. The particular defect-free nature and fluidity of DOPC monolayers/bilayers enabled very precise experiments to be carried out so that the factors promoting the interaction of aromatic compounds with phospholipid membranes can be better understood. Later studies would use more complex and more relevant model membrane systems.

Monolayers of phospholipids on the Hg surface act as a sensor element for aromatic compounds and many other species including biomembrane-active peptides and nanoparticle dispersions [22, 26-35]. At potentials around -0.4 V which is close to the position of zero charge (PZC) of Hg, the Hg supported DOPC monolayer is completely intact and impermeable to inorganic ions. At more negative potentials, capacitance peaks appear due to underlying field induced phase transitions occurring in the monolayer [36-39]. Alterations in the nature of these capacitance peaks are very sensitive to any changes in the monolayer structure. The capacitance peak occurring at around -0.94 V (capacitance peak-1) is associated with electrolyte penetration of the monolayer. The capacitance peak at around -1.0 V (capacitance peak-2) represents a phase transition involving a nucleation and growth process that results in the formation of a bilayer in equilibrium with electrolyte on the Hg surface. The described profile is specific to the capacitance-potential curves for DOPC monolayers. Different capacitance-potential profiles are obtained with different phospholipid

molecules [40]. The capacitance-potential profile is itself a fingerprint for a specified phospholipid monolayer. Interaction of organic compounds with the monolayer significantly influences the capacitance-potential profile of the layer in a selective and systematic manner. It has been established by direct imaging that binding of SiO$_2$ nanoparticles [34] to the DOPC polar groups elicits significant depression of the capacitance current peaks in proportion to the extent of binding. In addition it is clearly stated in other work [28-30] that the decrease in the DOPC capacitance peak-1 may be due to an interaction of the peptide with the DOPC polar heads and to an intercalation of the peptide between the hydrocarbon tails or to a possible combination of the two effects.

Phospholipid vesicles have been used extensively as a biological membrane mimic [41] to study the interactions of membrane active compounds [42,43] with membranes. The BPs have fluorescent properties which allow the use of fluorescence spectroscopy to estimate their fractions which have not penetrated into biomimetic assemblies such as phospholipid vesicles and are thus available for quenching by a quencher (e.g. I⁻) [44-47]. This is defined as the accessible fraction in this study. These experiments were carried out as a corollary to the electrochemical experiments to substantiate the nature of the BP-DOPC interactions. Table 1 summarizes the BP derivatives used in this study and their physical properties including log P values [48] and Hammets constants [49].

2. Experimental

2.1. Materials

o-chlorobiphenyl (o-Cl-BP), m-chlorobiphenyl (m-Cl-BP), p-chlorobiphenyl (p-Cl-BP), o-hydroxybiphenyl (o-HO -BP), m-hydroxybiphenyl (m-HO-BP), p-hydroxybiphenyl (p-HO-BP), p-methoxybiphenyl (p-H$_3$CO-BP), p-methylbiphenyl (p-H$_3$C-BP), p-cyanobiphenyl (p-NC-BP) and p-sulphonic acid biphenyl (p-HO$_3$S-BP) were purchased from Sigma Aldrich and their stock solutions (1000 ⌈mol dm^{-3}) were prepared in acetone and ethanol for electrochemical and fluorescence

studies respectively. p-HO$_3$S-BP exists in ionised form at the solution pH of 7.4 because its pK$_a$ value is near to that of toluene suphonic acid   [50] (~2.8) and is represented as p-O$_3$-S-BP throughout the text. The electrolyte, 0.1 mol dm^{-3} KCl was prepared from KCl (Fisher Chemicals Ltd.) calcined at 600 °C in a muffle furnace and dissolved in 18.2 M∧ MilliQ water containing 0.001 mol dm^{-3} phosphate buffer at pH 7.4. A 2.54 mmol dm^{-3} DOPC (Avantilipids) solution in pentane (HPLC grade, Fisher Scientific Chemicals Ltd.) was prepared for electrochemical experiments and a 12.7 mmol dm^{-3} stock DOPC dispersion in 0.1 mol dm^{-3} KCl containing 0.001 mol dm^{-3} phosphate buffer was used for preparation of vesicles in the fluorescence studies. An 8.0 mol dm^{-3} stock solution of KI (Fisher Scientific Ltd.) was prepared with 0.2 mmol dm^{-3} sodium thiosulphate (Na$_2$S$_2$O$_3$) in 18.2 M∧ MilliQ water for use in quenching experiments.

2.2. Electrochemical methods

2.2.1. Apparatus and procedure

The experiments were performed in a standard three electrode electrochemical cell containing; a Ag/AgCl, 3.5 mol dm^{-3} KCl as reference electrode with porous sintered ceramic frit separating the 3.5 mol dm^{-3} KCl solution from the electrolyte solution, a platinum rod as a counter electrode and a DOPC coated MFE as working electrode. The electrochemical apparatus was contained in a Faraday cage. The Hg film electrode (MFE) was prepared using a micro-fabricated Pt electrode (Tyndall National Institute, Ireland) having a 1 mm Pt disc area and a contact pad [24,31,32]. Fabricated electrodes were rinsed with with acetone and then MilliQ water,placed in in hot Piranha solution for 10-15 minutes, subsequently rinsed with MilliQ water and and dried under N$_2$ gas. Hg was deposited using an Eppendorf pipette on the Pt disc electrode to cover the Pt completely and the fabricated electrode inserted into electrochemical cell. A potential excursion from -0.2 to -3.0 V at 40V s^{-1} was used to remove organic material from the surface. The area (~0.009 mm^2) of the Hg was determined   from the capacitance-potential plot of the clean Hg surface as described previously. This electrode is stable and operational for up to three months [51].

The electrochemical cell, electrodes and all other glass apparatus were washed with Piranha solution to remove organic contamination. Subsequently, the apparatus and the electrodes were rinsed with MilliQ water to remove traces of Piranha residue. A PGSTAT 30 Autolab potentiostat (Ecochemie, Utrecht, Netherlands) interfaced to PowerLab 4/25 signal generator (AD Instruments Ltd.) controlled by Scope software was used to record rapid cyclic voltammetry (rcv) scans. The Autolab systems GPES (general purpose electrochemical studies) and FRA (frequency response analyser) with PGSTAT 30 and controlled with Autolab software were used for the alternating current voltammetry (acv) and impedance measurements respectively. The electrolyte solution was purged with argon gas for about 15-20 minutes followed by a redirection of argon gas as a blanket on top of electrolyte during the experiment. DOPC monolayers were prepared by spreading about 15 μcm^3 of 2.54 mmol dm^{-3} DOPC in pentane at the argon-electrolyte interface in the electrochemical cell. A period of 5-10 minutes was required for the pentane to evaporate. The MFE electrode was vertically lowered into the solution slowly through the interface to allow the DOPC monolayer to self-assemble on the Hg surface. Current-potential and impedance scans were recorded using electrochemical techniques. The MFE was cleaned by applying a cycling potential from -0.2 to -3.0 V to remove the DOPC monolayer and a new monolayer was deposited prior to each series of experiments. For electrochemical studies of substituted BP interactions, calculated amounts of their respective stock solution were injected below the DOPC monolayer into the electrolyte followed by gentle stirring of the solution for 5 minutes. Subsequent electrochemical analysis was then performed on the modified lipid coated electrode.

2.2.2. Rapid cyclic voltammetry (rcv)

rcv was used to acquire rapid scans and examine the properties of the monolayer at a scan rate (ν) of 40 Vs^{-1} with a potential excursion between -0.2 and -1.2 V on the DOPC coated Hg electrode.

The specific capacitance defined as the capacitance per unit area is related to the current (I) from rcv scans by the following equation:

$$C_{sp} = I/\acute{\jmath} A \qquad\qquad (1)$$

Suppression of the capacitance current peaks in the pure electrolyte solution may indicate either imperfections in the monolayer or the presence of contamination in the electrolyte solution. The electrode area, A, was estimated from the capacitance of the uncoated Hg [40].

2.2.3. Electrochemical impedance

Alternate current voltammograms (acv) were recorded by measuring the out-of-phase current in response to application of an ac sine wave of 0.005 V amplitude and 75 Hz frequency (f) added to a negatively increasing (ramp rate 5 mVs^{-1}) DC potential (E) from -0.2 to -1.2 V. C_{sp} was calculated using the current from the acv scans by the following equation:

$$C_{sp} = I/A\rceil\otimes V \qquad\qquad (2)$$

where $\rceil = 2\square f$ is the angular frequency and ΔV is the amplitude of the sine wave. At least three C_{sp}-E curves were recorded following fresh DOPC depositions on the MFE for each experiment. Measurements of the real and imaginary impedance of the electrode system using frequencies logarithmically distributed between 65000 to 0.1 Hz, with ac amplitude of 0.005 V and at potential -0.4 V (~PZC of Hg [52]) were carried out both in the absence and presence of BPs in the electrolyte solution. The real and imaginary impedance was normalized at respective frequencies and transformed to the complex capacitance plane as "Cole-Cole" plots using Microsoft EXCEL spreadsheet. Complex plane axes were expressed as Y'/ωA vs. Y''/ωA where Y'/ωA and Y''/ωA represent real and imaginary normalised admittances respectively divided by electrode area (A) as defined previously [53]. Incidentally, the series combination of a capacitance, C, and a resistance, R, which is simulated by the Hg-supported DOPC monolayer, is such that Y''/ωA equals $C/(\omega^2 R^2 C^2 + 1)A$, while Y'/ωA equals $\omega RC(Y''/\omega)/A$; moreover, the Y'/ωA vs. Y''/ωA plot yields a semicircle of diameter C/A and centre of coordinates (C/2A). This value C/A is frequency

8

independent and its value is extracted from measurements carried out over the whole frequency range from 10^5 to 0.1 Hz. This frequency independent capacitance (C/A) approximates to the monolayer capacitance divided by electrode area which is directly related to the monolayer dielectric permittivity and inversely related to the monolayer thickness. In this study the C/A was graphically determined from the complex capacitance plots and expressed as specific frequency independent capacitance (FIC$_{sp}$). In the case of the phospholipid coated Hg electrode, any additional circuit element (second semicircle and "tail") at lower frequencies outside of RC is reflective of ionic penetration [54] and physical modifications of the phospholipid monolayer respectively [53].

2.3. Fluorescence Spectroscopy

2.3.1. Principle

The basic principle in fluorescence spectroscopy involves the emission of light as a result of singlet-singlet electronic relaxation subsequent to absorbing light energy. The fluorescence has a typical life time of nanoseconds. In fluorescence spectroscopy, an incident light beam (usually UV) excites the electrons in the fluorophore molecule to the excited electronic states. These excited molecules then lose vibrational energy to return to the lowest vibrational state of the excited electronic state. As a result, the emission spectrum is recorded keeping the excitation wavelength constant and measuring the fluorescent light at different wavelengths. In this study, the substituted BP acted as an effective fluorophore [55]. The penetration of the BP into the vesicle bilayer was followed by recording the extent of quenching of the BP's fluorescence by KI (i.e. Γ as active quencher) which itself at lower solution KI concentrations did not penetrate the phospholipid bilayer. BPs which remained in the polar region of the bilayer were accessible to quenching by KI. BPs which penetrated the bilayer have their fluorescence quenched to varying degrees depending on their extent of penetration.

2.3.2. Preparation of liposomes

9

A DOPC stock dispersion of 12.7 mmol dm^{-3} was prepared by directly dispersing DOPC in 0.1 mol dm^{-3} KCl with added 0.001 mol dm^{-3} phosphate buffer. Unilamelar vesicles containing 3.9% ethanol and 0.249 mmol dm^{-3} DOPC were prepared by a modification of the solvent exchange procedure [56]. This involved adding 2 cm^3 of the DOPC stock dispersion to 4 cm^3 ethanol in a measuring flask followed by the addition of 96 cm^3 of 0.1 mol dm^{-3} KCl with added 0.001 mol dm^{-3} phosphate buffer gently along the wall of flask with constant swirling. The resulting vesicles formed a unidisperse dispersion of ~220 nm diameter unilamellar vesicles as characterised by dynamic light scattering (DLS) and confocal microscopy (not shown) and were found to be stable for up to 24 hours (Figure 1(a)). No attempt was made to remove the 3.9% ethanol from the dispersion since the ethanol facilitated the stability of the added biphenyl in solution for the subsequent fluorescence measurements. It has been shown that 4% ethanol does not significantly influence dimyristoyl PC (DMPC) conformation in vesicle dispersions [57] and shows no significant interaction with DOPC monolayers supported on Hg (data not shown).

2.3.3. Instrumentation and procedure

A FluoroMax-3 Fluorimeter from Horiba Scientific with xenon lamp was used to obtain fluorescence spectra. Fluorescence spectra of DOPC vesicles at the excitation wavelengths specific to different BPs were recorded as controls. Substituted BP solutions were added to the DOPC vesicle dispersions to a concentration of 1 ⌈mol dm^{-3} with an incubation period of 15 minutes before measurement. KI was used as a quencher. Secondary stock solutions of different concentrations of KI (1.0-7.0 mol dm^{-3}) were prepared from the primary stock solution of 8.0 mol dm^{-3} KI and 0.2 mmol dm^{-3} Na$_2$S$_2$O$_3$ in 18.2 M∧ MilliQ water. Na$_2$S$_2$O$_3$ was used as a reducing agent to prevent the oxidation of iodide to iodine. 0.15 cm^3 portions of the KI secondary stock solutions were added to the 3 cm^3 of vesicle dispersion containing substituted BPs in the cuvette to give 0.047 to 0.333 mole dm^{-3} KI concentrations and fluorescence spectra were recorded at appropriate excitation and emission wavelengths. The cuvette was dried from inside using

compressed air before taking all the measurements to eliminate the error from small dilutions. Maximum fluorescence intensities were measured from the fluorescence spectra. All fluorescence spectra were corrected for the fluorescence of a vesicle dispersion with no biphenyl and no quencher. An example of a corrected fluorescence spectrum is shown in Figure 1(b). Fluorescence data were plotted versus the inverse of the KI concentration according to the modified Stern-Volmer equation [44].

$$F^{\circ}/\otimes F = (1 / f_a K c_{KI}) + 1/f_a \qquad (3)$$

Where F^o is the intensity of emitted light in the absence of quencher and ΔF is the difference in the intensities of emitted light in the absence and presence of quencher respectively, K is the Stern-Volmer quenching constant, c_{KI} is the KI concentration and f_a is the accessible fraction. The accessible fraction is defined as the fraction (expressed in text as %) of the fluorophore present in the polar region of the DOPC bilayer and hence available for quenching. The accessible fraction therefore reports on the location of the BP fluorophore in the membrane. The accessible fractions (f_a) for the quenching of the BP derivative fluorescence were calculated from the intercept values (intercept = $1/f_a$) with an intercept value of 1.0 indicating 100% accessibile fraction of the BP derivatives to quenching by I^-. The slope of these plots gives the effective quenching constant (K) for accessible fluorophores which is similar to the binding constant for the quencher-acceptor systems [58] and represents the quenching efficiency of the BP derivatives by I^-. It is not a significant parameter in terms of their interaction with the membrane. 0.04 mmol dm^{-3} I^- has been shown to interact with the polar but not penetrate the apolar region in Hg supported DOPC monolayers [54] and is known to associate with the choline group of DOPC [59]. Indeed it was shown from I^- quenching of Laurdan (6-dodecanoyl-2-dimethylaminonaphthalene) in the DOPC phospholipid bilayer that I^-, from solution concentrations above 0.15 mol dm^{-3}, penetrates down to the glycerol level of the phospholipid bilayer [59].

In this study all experiments were carried out under the same conditions thus it is unlikely that the I⁻/DOPC interaction will affect the relative BP penetration into the membrane. This asssumption is supported by the characteristic Stern-Volmer plot (Figure 1(c)) where the slope of the plot is linear indicating that the increase in I⁻ concentration is not affecting the BP accessible fraction and hence BP penetration. However, at higher solution concentrations of I⁻, a discrete increase in the slope of the modified Stern-Volmer plots was observed. This increase in slope is due to the I⁻ penetrating the apolar region of the monolayer and quenching penetrated BP. This data is therefore excluded from the plot used to estimate the intercept. All the BP derivatives were found to be stable on exposure to light (constant intensity of re-emitted light on repetitive exposure to light) except o-Cl-BP and were studied using the method described above. For o-Cl-BP, the spectra were recorded in kinetic acquisition mode with an interval of 0.1 s and 6 s total time, at an excitation wavelength of 260 nm and an emission wavelength of 316 nm to eliminate the effects from photo-degradation. The intercept from the linear regression of these intensity values versus time yielded the intensity of re-emitted light at zero time (where there is no photo degradation) and was used to plot the modified Stern-Volmer plot for I⁻ quenching of o-Cl-BP.

3. Results and discussion

The effect of the interaction of the substituted mono HO-BPs with the DOPC monolayer on the capacitance-potential plot is shown in Figure 2(a). Suppression of the peak-1 capacitance with an increase in solution concentration of o-, m- and p-HO- BPs is clear and the extent of suppression follows the order of o-<m-<p- HO-BP/DOPC interaction (Figure 2(b)). This suppression of the capacitance peak is directly related to the extent of interactions of these BPs with the DOPC monolayer [22,27] indicating that the p-HO-BP showed the strongest interactions with the DOPC monolayer compared to that of m- and o-HO-BP. Notably the potentials (-E) characterising capacitance peaks-1 and -2 do not markedly change on penetration of the HO-BP into the monolayer. The accessible HO-BP fraction for I⁻ quenching in the presence of vesicles prepared

12

from a 0.249 mmol dm^{-3} DOPC dispersion indicates that this fraction is lowest for p-HO-BP and increases in the following order: p-HO-BP (17.21 %) < m-HO-BP (29.03 %) < o-HO-BP (90.63 %) which indicates the penetration extent of HO-BP into the apolar core is in the order: p-HO-BP (82.79 %) > m-HO-BP (70.97%) > o-HO-BP (9.37%). This order arises from: (i) the symmetrically linear and planar structure of the p-isomer enabling its ready penetration into the apolar membrane core; (ii) the lack of two-fold symmetry of the m-isomer rendering it less able to penetrate the phospholipid membrane; and, (iii) the twisted geometry of the o-isomer arising from the increased torsion angle between the two phenyl rings further impeding its penetration.

The capacitance peak-1 height correlates with the accessible fraction of HO-BPs for quenching (Figure 2(c)) indicating that the fluorescence results are commensurate with and support the electrochemical results and together relate qualitatively to the interaction of the HO-BP with the DOPC layer. This suggests that the HO-BPs behave in a comparable manner at the Hg supported monolayer/electrolyte interface and at the vesicle/electrolyte interface. Figure 2(d) shows the impedance data represented as a complex capacitance plot of a DOPC coated Hg electrode in the presence of o-, m- and p-HO-BPs. In this plot the interaction of these species with the DOPC monolayer is represented by the presence of a low frequency "tail" at the right hand side of the plot. The frequencies defining this tail are lower than ~22 radians s^{-1} and are usually representative of imperfections in the layer and species adsorbed within the DOPC [53]. It is interesting that the monolayer capacitance does not decrease following the interaction of DOPC with the HO-BP isomers and the interaction of p-HO-BP with DOPC and its penetration introduces an additional very small irregular semicircular element defined by frequencies 1900 to 13 radians s^{-1} between the RC element and the "tail". The inset to Figure 2(d) shows this intermediate circuit element more clearly. Current work investigating the interaction of small molecular weight organic compounds with DOPC layers show that phenolic compounds tend to have a disruptive effect on DOPC monolayers compared to non-polar aromatics. This intermediate circuit element could relate to the

disruptive effect of the p-HO-BP leading to ionic penetration within the polar head region [54]. Further more focused work would need to be carried out to establish this.

Interaction of Cl-BPs with DOPC monolayers on Hg had a significant effect on the capacitance-potential plot (see Figure 3 (a)). Suppression of the peak-1 capacitance with an increase in solution concentration of o-, m- and p-Cl-BPs is clear (Figure 3(b)) and following interaction of the Cl-BPs with the DOPC monolayer, the capacitance peak suppression was more pronounced compared to that following HO-BP/DOPC interactions (Figure 3(a) and (b) compared to Figures 2(a) and (b)). This observation indicates that Cl-BP interacts more strongly than HO-BP with the DOPC polar heads. This shows a deeper penetration of HO-BP than Cl-BP in the DOPC layer. In addition, capacitance peak-1 and more extensively peak-2 (Figures 3 (a)) were shifted to more negative potentials in the presence of m- and p-Cl-BPs. The accessible Cl-BP fraction for I^- quenching in the presence of vesicles prepared from a 0.249 mmol dm^{-3} DOPC dispersion showed that this fraction increased in the following order: p-Cl-BP (76.47 %) < m-Cl-BP (93.14 %) < o-Cl-BP (96.08 %). This indicates that the extent of penetration of Cl-BP into the monolayer apolar core is in the order: p-Cl-BP (23.53 %) > m-Cl-BP (6.86 %) > o-Cl-BP (3.92%). The isomers of Cl-BPs exhibited a similar order of incorporation/penetration into the bilayer to that of HO-BPs but the extent of the penetration is decreased which is commensurate with the capacitance peak suppression results above. Cl-BPs have a comparable 3D structure to their HO- analogues but there is an essential difference in distribution of electron density among the ring atoms in these substituted BPs. It is well established that the HO- group acts as an electron donor but the Cl- group acts as an electron acceptor when attached to aromatic rings. This is described by Hammetts substitution constant ($\int_t$) [49] (see Table 1) of the functional group attached to an aromatic ring where negative and positive values indicates the substituent is electron donating and withdrawing respectively relative to H-. Accordingly HO-BP has an increased ring electron density than Cl-BP and penetrates the DOPC bilayer to a greater extent than Cl-BP. In Figure 3(c) it can be seen that the capacitance peak-1

height from the capacitance-potential plot of a DOPC monolayer on Hg correlates with the Cl-BP accessible fraction for quenching in DOPC vesicle dispersions. This indicates that the fluorescence results are commensurate with and support the electrochemical results together relating to the extent of interaction of the Cl-BP with the DOPC layer.

Figure 4(a) displays the impedance plots of the DOPC coated Hg electrode in the presence of Cl-BPs in the electrolyte solution. It is clear from the presence of the low frequency "tail" on the right hand side of the plot, that the Cl-BPs interact with the DOPC monolayer. Figure 4(b) displays the FIC_{sp} versus Cl-BP concentration plots and it can be seen that the monolayer capacitance decreases in the presence of Cl-BPs in solution. In fact the following order of FIC_{sp} decrease subsequent to interaction of the following Cl-BP s with the DOPC monolayer is: p-Cl-BP > m-Cl-BP > o-Cl-BP commensurate with the degree of interaction of these componds with the DOPC monolayer. If it is assumed that the relative permittivity of Cl-BPs (~5-6 [60,61]) is about two times higher than that of the hydrocarbon layer of the monolayer, a decrease in monolayer capacitance clearly indicates the formation of a thicker monolayer. Indeed, the increase in monolayer thickness must be the over-riding factor leading to a decrease in FIC_{sp}. Furthermore, the negative shift of the capacitance peaks associated with Cl-BP/DOPC interaction can be related to the increasing thickness of the low dielectric region. This increases the applied potential required for the instigation of the phase transition underlying the capacitance peak (Figure 3 (a)) enabling the phase transition to take place at the critical field value [62]. A further explanation for the peak shift is that the polarizability of the aromatic rings (assumedly located in the polar group region) lessens the steepness of the potential drop across the layer [62]. This leads to a greater applied potential to be used to initiate the phase transitions.

Figure 5(a) plots the BP substituent $\int_t$ values against the substituted BP accessible fraction in the membrane for all substituted BP/DOPC membrane interactions. It is significant that p-H$_3$C-BP and

15

p-O$_3^-$S-BP are significant outliers on this plot. The σ_t values employed have been calculated for substituted benzenes and include both long range mesomeric (σ_m) and short range inductive (σ_t-σ_m) effects of substitution [63]. The benzene molecule is small and the inductive effect is significant in changing its properties but in the case of BP and other larger molecules, the inductive effect does not extend to the unsubstituted ring   compared to the mesomeric effect [64]. In order to estimate the precise and realistic electron density on the unsubstituted BP ring, mesomeric Hammetts constants σ_m [49] were used. Figure 5(b) shows the correlation between the substituted BP accessible fraction and σ_m of the substituent. The substituent value of σ_m generally showed a good correlation with the accessible fraction of BPs subject to I^- quenching.   p-O$_3^-$S-BP is a marginal outlier to this trend but it is a negatively charged molecule with a large polar O$_3^-$S- group which will additionally favour its preference for the polar region. Figure 6 shows a plot of the FIC$_{sp}$ extracted from the complex capacitance plots of BP penetrated DOPC on Hg versus the accessible fraction of substituted BPs subject to I^- quenching in the presence of DOPC vesicles. The V shaped plot shows a minimum FIC$_{sp}$ representing a maximum thickness of the DOPC corresponding to the intermediate value of the accessible fraction. An outlier to the trend is the point representing the o-HO-BP/DOPC interaction which could be due to a variety of factors and requires further investigation. The accessible fraction is in inverse proportion to the penetration depth of the substituted BP in the bilayer membrane and, assuming that the penetration of BPs in the monolayer and bilayer are the same or similar, the mid-location of the Cl-BP in the monolayer is related to a maximum thickness of the monolayer. By the same token, when the substituted BP is located outside this region either nearer to the surface of the monolayer or deeper in the apolar core, the increase in thickness is not so pronounced.

4. Model

The experimental observations support a model whereby NC-BP is located within the DOPC polar head region, Cl-BP is located at the DOPC polar-apolar interface and HO-BP is located towards the

DOPC apolar core. The model is commensurate with the existence of CH-$\square$ associations in which a significant contribution comes from dispersion interactions [65] favoured by the increased electron density or polarizability of the aromatic ring [65,66]. This is facilitated by electron donating substitutuents (eg for HO-, σ_t- σ_m = -0.37 and σ_m = -0.735) on the biphenyl aromatic rings which will enable deeper insertion of the biphenyl rings into the apolar core. The model is also substantiated by the existence of H-bonding between the substituted BPs and the DOPC molecules. In the case of aromatic rings acting as electron donors, this interaction favours CH-$\square$ association where the acyl chain >CH- group is the electron acceptor [67,68]. On the other hand the aromatic ring can act as acceptor in the presence of electron withdrawing substituents [69]. A particular example of this is pentafluorobenzene which forms H-bonds due to the electron withdrawing effect of the F- substituents [70]. These effects would favour interactions between electron withdrawing (eg for NC-, σ_t- σ_m = 0.66 and σ_m = 0.15 [49]) substituted biphenyl aromatic rings and the DOPC polar group region.

The Cl- substituent of p-Cl-BP has a strong inductive electron accepting effect (σ_t- σ_m = 0.42 [49]) and a weak mesomeric electron donating effect (σ_m = -0.19) which renders the substituted BP ring relatively more electron deficient than the unsubstituted ring. This is because the inductive effect only operates on the substituted ring [64]. This difference in electron density of the substituted and unsubstituted rings respectively leads to a directional location of p-Cl-BP in the DOPC layer. The unsubstituted ring remains in the apolar region through CH-$\square$ interactions whereas the substituted ring tends towards the apolar/polar interface. Such a structure can be stabilized by a halogen bond between Cl- of p-Cl-BP and the phosphate group oxygen [71,72] of PC. The head groups of DOPC in the liquid phase of the monolayer are oriented parallel to the layer plane [73,74] whereas the apolar tails of DOPC molecule are in a plane normal to the monolayer. As a result, the positioning of the rigid p-Cl-BP in the right-angled interfacial region will increase the angle between the polar

groups and the alkyl chains and cause a thickening of the layer as observed from the capacitance decrease in Figure 4(b).

The propensity for the substituted BPs to form H-bonds with the polar DOPC moieties has been explored. This is a semi-quantitative exercise which has been carried out to substantiate the conclusions from the preceding experiments. It is acknowledged that a more complete treatment, outside the scope of this paper, would take account of the water molecular environment. H-bonding energies of substituted BPs with the glycerol-dicarboxylic ester moiety of DOPC have been estimated. Methyl acetate (CH_3-(CO)O-CH_3) was chosen as a molecule to model the glycerol-dicarboxylic ester grouping of DOPC and its binding with the substituted BPs. The choice of methyl acetate is justified since its structure is analagous to each of the two parts of the glycerol-dicarboxylic ester of DOPC namely R-(CO)O-CH< and R-(CO)O-CH_2- where R- is the oleoyl chain. It is to be noted that the binding energy between p-X-BP (where X is the substituent) to methyl acetate is half that of the binding energy of two p-X-BP molecules with each of the two ester groups of one DOPC molecule. The critical H-bonding moieties in both the methyl acetate molecule and the glycerol-dicarboxylic ester fragment are C-O-C and >C=O. Binding energies were also estimated between the >C=O (methyl acetate) and HO- (p-HO-BP) groups and between the -PO_2^-- (DOPC) and Cl- (p-Cl-BP) groups to substantiate the conclusions. All energies were calculated using the program package Jaguar from Schrodinger, Inc. (Maestro Version 10.2.011, MMshare Version 3.0.011, Release 2015-2, Platform Windows-x64) and are displayed in Tables 2 and 3. The binding energy between two water molecules was calculated with the same program in order to compare it with the other estimated binding energies.

Table 2 shows complexes of unsubstituted and substituted BPs with CH_3-(CO)O-CH_3. Complex A exhibits two hydrogen bonds between the m- and p- hydrogens of the unsubstituted BP ring and the C-O-C and >C=O oxygens respectively of CH_3-(CO)O-CH_3. Complex B exhibits: (a) two

hydrogen bonds between the o- hydrogens of the substituted and unsubstituted BP rings and the >C=O oxygen of CH_3-(CO)O-CH_3 and, (b) a hydrogen bond between the m-hydrogen of the substituted BP and the C-O-C oxygen of CH_3-(CO)O-. Table 2 lists the binding energies calculated for complexes between the BPs and CH_3-(CO)O-CH_3. Complexes A and B with unsubstituted BP show similar binding energies. The Complex B of p-Cl-BP shows a higher binding energy of 2.27 compared to 1.8 kcal mol^{-1} for Complex A. The preferable formation of Complex B would result in the positioning of the unsubstituted phenyl ring inside the apolar region of DOPC layer and the substituted phenyl ring in the interfacial layer of DOPC. The bonding of Cl- with the DOPC -PO_2^-- grouping with an energy of 2.08 kcal mol^{-1} (see Table 3) would re-enforce this structure. Binding energies of p-HO-BP with CH_3-(CO)O-CH_3 are 1.31 and 1.03 kcal mol^{-1} for Complexes A and B respectively. This is more than offset by the relatively high binding energy of HO- with the methyl acetate, >C=O group, of 7.43 kcal mol-1 (see Table 3) which has a higher energy than the HOH-HOH bond energy (5.05 kcal mol-1). This favours the positioning of both p-HO-BP rings within the apolar core of DOPC. The binding of p-NC-BP rings with CH_3-(CO)O-CH_3 favours Complex A (2.86 kcal mol^{-1}). The relatively high binding energy in this case is enabled by the electron withdrawing NC- group. The bonding of the unsubstituted ring and the high polarity of the NC- group [75] will promote the positioning of the p-NC-BP substituted ring within the polar head region of the DOPC layer.

5. Conclusions

The interaction of monosubstituted BPs with DOPC bilayers and monolayers is strongly dependent on the structural and electronic configuration of the molecules and specifically:-.

1. p-substituted BPs compared to o- and m-substituted BPs exhibit stronger interactions with DOPC bilayers and monolayers because of retained co-planarity of the two aromatic rings irrespective of the nature of substituent.

2. BPs with electron donor substituents penetrate the apolar core of the bilayer whereas BPs with electron acceptor substituents are incorporated in the polar group region of the DOPC bilayer. BPs located at the interface between the polar and apolar region increase the DOPC monolayer thickness.

3. Experimental results and binding energy calculations indicate that the three structural and electronic features influencing the location of substituted BPs in DOPC bilayers and monolayers are respectively: (i) The position of the substituent, (ii) the electron density or polarizability of the BP rings and, (iii) the hydrogen bonding capability of the aromatic rings.

4. Both electrochemical and fluorescence studies exhibit a consistent pattern of interactions between substituted BPs and DOPC bilayers and monolayers respectively suggesting that the Hg electrode support has an insignificant influence on the interactions of the substituted biphenyl compounds with DOPC.

These findings are directly relevant to the initial objective of the work in that they relate the molecular properties of substituent position and ring polarizability to the extent of interaction of the substituted biphenyl with phospholipid monolayers/bilayers as a model for biological membranes. This has important relevance to biological membrane function not only with respect to the interaction of aromatic pharmaceuticals with biomembranes but also in relation to the conformation of proteins containing aromatic rings within biomembranes. In both cases the biomembrane structure, function and biomolecular organization is strongly affected by the nature of the aromatic ring/biomembrane associations.

6. Acknowledgments

7. References

[1] J.I.Kroschwitz, M.Howe-Grant, Kirk-Othmer Concise Encyclopedia of Chemical Technology, Wiley New York, 1999.

[2] S.Bonora, A.Torreggiani and G.Fini, DSC and Raman study on the interaction between polychlorinated biphenyls (PCB) and phospholipid liposomes, Thermochimica acta 408 (2003) 55.

[3] H. S. D. Bank, National Library of Medicine, National Toxicology Information Program, Bethesda, MD (USA), 1994.

[4] US Environmental Protection Agency, Toxicological Review of Biphenyl, EPA/635/R-11/005F, 2013.

[5] J.Borja, D.M.Taleon, J.Auresenia and S. Gallardo, Polychlorinated biphenyls and their biodegradation, Process Biochemistry 40 (2005) 1999.

[6] O.Hutzinger and J. Paasivirta, New Types of Persistent Halogenated Compounds, Handbook of Chemistry, Springer-Verlag, Berlin, Vol. 3, 2000.

[7] R.E.Billings, R.E.McMahon, Microsomal biphenyl hydroxylation: the formation of 3-hydroxybiphenyl and biphenyl catechol, Molecular Pharmacology 14 (1978) 145.

[8] K.L.Kaiser and P.T.Wong, Bacterial degradation of polychlorinated biphenyls, Bulletin of Environmental Contamination and Toxicology 11 (1974) 291.

[9] E.K.Wehler, L.Hovander and B-O. Lund, 2,2',4,5,5'-pentachlorobiphenyl: Comparative metabolism in mink (Mustela vison) and mouse, Chemical Research in Toxicology 9 (1996) 1340.

[10] E.K.Wehler, L.Lindberg, C-J. Jönsson and Å. Bergman, Tissue retention and metabolism of 2,3,4,3′,4′-pentachlorobiphenyl in mink and mouse. Chemosphere 27(1993) 2397.

[11] A.Bergman, E.K.Wehler and H.Kuroki, Selective retention of hydroxylated PCB metabolites in blood, Environmental Health Perspectives 102 (1994) 464.

[12] Sandanger, T. M.; Dumas, P.; Berger, U.; Burkow, I. C. Analysis of HO-PCBs and PCP in blood plasma from individuals with high PCB exposure living on the Chukotka Peninsula in the Russian Arctic. Journal of Environmental Monitoring, 2004, 6, 758.

[13] A.Brouwer, D.C.Morse, M.C.Lans, A.G.Schuur, A.J.Murk, E.K.Wehler, Å. Bergman and T.J.Visser, Interactions of persistent environmental organohalogens with the thyroid hormone system: mechanisms and possible consequences for animal and human health, Toxicology and Industrial Health 14 (1998) 59.

[14] M.C.Lans, E.K.Wehler, M.Willemsen, Meussen, E.; Safe, S.; Brouwer, A. Structure-dependent, competitive interaction of hydroxy-polychlorobiphenyls, -dibenzo-p-dioxins and -dibenzofurans with human transthyretin, Chemico-Biological Interactions 88 (1993) 7.

[15] Y.Takei, T.Yamaguchi, Y.Osamura, K.Fuke and K.Kaya, Electronic spectra and molecular structure of biphenyl and para-substituted biphenyls in a supersonic jet, The Journal of Physical Chemistry 92 (1988) 577.

[16] O.Bastiansen and S.Samdal, Structure and barrier of internal rotation of biphenyl derivatives in the gaseous state: Part 4. Barrier of internal rotation in biphenyl, perdeuterated biphenyl and seven non-ortho-substituted halogen derivatives. Journal of Molecular Structure 128 (1985) 115.

[17] Y.Tan, D.Li, R.Song, D.Lawrence and D.O.Carpenter, Ortho-substituted PCBs kill thymocytes, Toxicological Sciences 76 (2003) 328.

[18] Y.Tan, R.Song, D.Lawrence and D.O.Carpenter, Ortho-substituted but not coplanar PCBs rapidly kill cerebellar granule cells. Toxicological Sciences 79 (2004) 147.

[19] Y.Tan, C-H.Chen, D.Lawrence and D.O.Carpenter, Ortho-substituted PCBs kill cells by altering membrane structure, Toxicological Sciences 80 (2004) 54.

[20] J.M.Cullen and K.L.Kaiser, An examination of the role of rotational barriers in the toxicology of PCB's, in K.L.Kaiser (Ed), QSAR in Environmental Toxicology, Springer, Netherlands, 1984, p 39.

[21] A.M.Bobra, W.Y.Shiu and D.Mackay, Structure-activity relationships for toxicity of hydrocarbons, chlorinated hydrocarbons and oils to Daphnia magna, in K.L.Kaiser (Ed), QSAR in Environmental Toxicology, Springer, Netherlands, 1984, p 3.

[22] A.Nelson, N.Auffret and J.Borlakoglu, Interaction of hydrophobic organic compounds with mercury adsorbed dioleoylphosphatidylcholine monolayers, Biochimica et Biophysica Acta (BBA)-Biomembranes 1021 (1990) 205.

[23] S.S. Deol, P. J. Bond, C. Domene and M. S. P. Sansom, Lipid-protein interactions of integral membrane proteins: a comparative simulation study, Biophysical Journal 87 (2004) 3737.

[24] K. M. Sanchez, G. Kang, B.Wu and J. E. Kim, Tryptophan-lipid interactions in membrane protein folding probed by ultraviolet resonance Raman and fluorescence spectroscopy, Biophysical Journal 100 (2011) 2121.

[25] A.G. Lee, Lipid–protein interactions in biological membranes: a structural perspective, Biochimica et Biophysica Acta 1612 (2003) 1.

[26] A.Nelson, Influence of biologically active compounds on the monomolecular gramicidin channel function in phospholipid monolayers, Langmuir 12 (1996) 2058.

[27] S.Mohamadi, D. J. Tate, A. Vakurov and A. Nelson, Electrochemical screening of biomembrane-active compounds in water, Analytica Chimica Acta 813 (2014) 83.

[28] L.Becucci, M.Innocenti1, S.Bellandi and R.Guidelli, Permeabilization of mercury-supported biomimetic membranes by amphotericin B and the role of calcium ions, Electrochim. Acta 112 (2013) 719.

[29] L. Becucci, D. Valensin, M. Innocenti, R. Guidelli, Dermcidin, an anionic antimicrobial peptide: influence of lipid charge, pH and Zn^{2+} on its interaction with a biomimetic membrane, Soft Matter 10 (2014) 616.

[30] L. Becucci, M.L. Foresti, A. Schwan and R .Guidelli, Can proton pumping by SERCA enhance the regulatory role of phospholamban and sarcolipin? Biochim. Biophys. Acta 1828 (2013) 2682.

[31] L.Ringstad, E.Protopapa, B.Lindholm-Sethson, A.Schmidtchen, A.Nelson and M.Malmsten, An electrochemical study into the interaction between complement-derived peptides and DOPC mono- and bilayers, Langmuir 24 (2008) 208.

[32] L. Ringstad, A. Aggeli and A. Nelson, Interaction of self-assembling β-sheet peptides with phospholipid monolayers: The effect of serine, threonine, glutamine and asparagine amino acid side chains, Electrochimica Acta 55 (2010) 3368.

[33] F Neville, D Gidalevitz, G Kale and A Nelson, Electrochemical screening of anti-microbial peptide LL-37 interaction with phospholipids, Bioelectrochemistry 70 (2) 205.

[34] A.Vakurov, R.Brydson and A.Nelson, Electrochemical modeling of the silica nanoparticle-biomembrane interaction, Langmuir 28 (2011) 1246.

[35] A.Vakurov, G.M.Lopez, R.Drummond-Brydson, R.Wallace, C.Svendsen and A.Nelson, ZnO nanoparticle interactions with phospholipid monolayers, Journal of Colloid and Interface Science 404 (2013) 161.

[36] A.Nelson and N.Auffret, Phospholipid monolayers of di-oleoyl lecithin at the mercury/water interface, Journal of Electroanalytical Chemistry and Interfacial Electrochemistry 244 (1988) 99.

[37] A.Nelson and F.A.M.Leermakers, Substrate-induced structural changes in electrode-adsorbed lipid layers: Experimental evidence from the behaviour of phospholipid layers on the mercury-water interface, Journal of Electroanalytical Chemistry and Interfacial Electrochemistry 278 (1990) 73.

[38] A.V.Brukhno, A. Akinshina, Z. Coldrick, A. Nelson and S. Auer, Phase phenomena in supported lipid films under varying electric potential, Soft Matter 7 (2011) 1006.

[39] A.Vakurov, M. Galluzzi∞, A.Podestà, N. Gamper, A. L. Nelson and S. D. A. Connell, Direct Characterization of Fluid Lipid Assemblies on Mercury in Electric Fields, ACS Nano 8 (2014) 3242.

[40] Z. Coldrick, P. Steenson, P. Millner, M. Davies, A. Nelson, Phospholipid monolayer coated microfabricated electrodes to model the interaction of molecules with biomembranes, Electrochim. Acta 54 (2009) 4954.

[41] J.H.Fendler, Surfactant vesicles as membrane mimetic agents: characterization and utilization, Accounts of Chemical Research 13 (1980) 7.

[42] M.Magzoub, K. Kilk, L.G.Eriksson, Ü.Langel and A.Gräslund, Interaction and structure induction of cell-penetrating peptides in the presence of phospholipid vesicles, Biochimica Et Biophysica Acta (BBA)-Biomembranes 1512 (2001) 77.

[43] K.Lohner, A.Latal, R.I.Lehrer and T.Ganz, Differential scanning microcalorimetry indicates that human defensin, HNP-2, interacts specifically with biomembrane mimetic systems. Biochemistry 36 (1997) 1525.

[44] S.S.Lehrer, Solute perturbation of protein fluorescence. The quenching of the tryptophyl fluorescence of model compounds and of lysozyme by iodide ion, Biochemistry 10 (1971) 3254.

[45] J.Dufourcq and J-F.Faucon, Intrinsic fluorescence study of lipid-protein interactions in membrane models. Binding of melittin, an amphipathic peptide, to phospholipid vesicles, Biochimica et Biophysica Acta (BBA)-Biomembranes 467 (1977) 1.

[46] C.Casals, E.Miguel and J. Perez-Gil, Tryptophan fluorescence study on the interaction of pulmonary surfactant protein A with phospholipid vesicles, Biochem. J. 296 (1993) 585.

[47] R.Fato, M.Battino, M.Degli Esposti, G.Parenti Castelli and G.Lenaz, Determination of partition and lateral diffusion coefficients of ubiquinones by fluorescence quenching of n-(9-anthroyloxy) stearic acids in phospholipid vesicles and mitochondrial membranes. Biochemistry 25 (1986) 3378.

[48] H.E.Pence and A.Williams, ChemSpider: An on-line chemical information resource. Journal of Chemical Education 87 (2010) 1123.

[49] C.Hansch, A.Leo and R. Taft, A survey of Hammett substituent constants and resonance and field parameters, Chemical Reviews 91 (1991) 165.

[50] J.P.Guthrie, Hydrolysis of esters of oxy acids: pKa values for strong acids; Brønsted relationship for attack of water at methyl; free energies of hydrolysis of esters of oxy acids; and a linear relationship between free energy of hydrolysis and pK_a holding over a range of 20 pK units, Canadian Journal of Chemistry 56 (1978) 2342.

[51] L. A. Nelson and Z. Coldrick, BIOSENSOR WO2009016366 A1, PCT Application No. PCT/GB2008/002591:priority filing 31.07.07. Granted by European office.

[52] D.Bizzotto and A.Nelson, Continuing electrochemical studies of phospholipid monolayers of dioleoyl phosphatidylcholine at the mercury−electrolyte interface, Langmuir 14 (1998) 6269.

[53] C.Whitehouse, R.O'Flanagan, B.Lindholm-Sethson, B.Movaghar and A.Nelson, Application of electrochemical impedance spectroscopy to the study of dioleoyl phosphatidylcholine monolayers on mercury, Langmuir 20 (2004) 136.

[54] J.Merrifield, J.Tattersall, M. Bird and A. Nelson, Interaction of bispyridinium compounds with phospholipid layers in presence and absence of electric field, Electroanalysis 19 (2007) 272.

[55] J.W.Bridges, P.J. Creaven and R.T.Williams, The fluorescence of some biphenyl derivatives, Biochem. J. 96 (1965) 872.

[56] Preparation of uniform-size liposomes and other lipid structures. US Patent WO1989 011335A1.

[57] L.Toppozini, C.L.Armstrong, M.A. Barrett, S.Zheng, L. Luo, H. Nanda, V.G. Sakai and M.C.Rheinstaedter, Partitioning of ethanol into lipid membranes and its effect on fluidity and permeability as seen by X-ray and neutron scattering, Soft Matter 8 (2012) 11839.

[58] M.Sharma, K.Chauhan, R. Shivahare, P.Vishwakarma, M.K.Suthar, A.Sharma, S.Gupta, J.K.Saxena, J. Lal and P. Chandra, Discovery of a new class of natural product-inspired quinazolinone hybrid as potent antileishmanial agents, Journal of Medicinal Chemistry 56 (2013) 4374.

[59] R.Vacha, P.Jurkiewicz, M. Petrov, M.L.Berkowitz, R.A. Boeckmann, J.Barucha-Kraszewska, M.Hof, M. and P. Jungwirth, Mechanism of interaction of monovalent ions with phosphatidylcholine lipid membranes, J. Phys. Chem. B 114 (2010), 9504.

[60] J.F. Ross, Handbook for radio engineering managers, Elsevier, Amsterdam, 2014.

[61] R.D.Kimbrough and A.A. Jensen (Eds), Halogenated biphenyls, terphenyls, naphthalenes, dibenzodioxins and related products, Volume 4, Elsevier, Amsterdam,2012.

[62] A.Rashid, A.Vakurov and A. Nelson, Role of electrolyte in the occurrence of the voltage induced phase transitions in a dioleoyl phosphatidylcholine monolayer on Hg, Electrochimica Acta 155 (2014) 458.

[63] C.K.Ingold, Principles of an electronic theory of organic reactions, Chemical Reviews, 15 (1934) 225.

[64] E.Schulman, K. Christensen, D.M.Grant and C.Walling, Substituent effects on carbon-13 chemical shifts in 4-substituted biphenyls and benzenes. Substituent effect transmitted through eight covalent bonds, The Journal of Organic Chemistry 39 (1974) 2686.

[65] S.Tsuzuki, CH/□ interactions, Annu. Rep. Prog., Chem., Sect. C: Phys. Chem., 108 (2012) 69.

[66] M.J.Plevin, D.L. Bryce and J. Boisbouvier, Direct detection of CH/□ interactions in proteins Nature Chemistry 2 (2010) 466.

[67] M.Nishio, Y.Umezawa, J. Fantini, M.S.Weiss, and P.Chakrabarti, CH–□ hydrogen bonds in biological macromolecules, Physical Chemistry Chemical Physics 25 (2014) 12648.

[68] M.Nishio, CH/□ hydrogen bonds in crystals, CrystEngComm. 6 (2004) 130.

[69] E.Arras, A.P. Seitsonen, F.Klappenberger, J.V. Barth, Nature of the attractive interaction between proton acceptors and organic ring systems. Physical Chemistry Chemical Physics 14 (2012) 15995.

[70] J.R.Murdoch and A.Streitwieser Jr., Hydrogen bonding between pentafluorobenzene and pyridine-d5, The Journal of Physical Chemistry 85 (1981) 3352.

[71] P.Auffinger, F.A.Hays, E. Westhof and P.S.Ho, Halogen bonds in biological molecules, PNAS 101 (2004) 16789.

[72] C.B.Aakeroy, M.Fasulo, N. Schultheiss, J. Desper and C.Moore, Structural competition between hydrogen bonds and halogen bonds. J. Am. Chem. Soc. 129 (2007) 13772.

[73] H.Hauser, I.Pascher, I., R.H.Pearson and S.Sundell, Preferred conformation and molecular packing of phosphatidylethanolamine and phosphatidylcholine, Biochimica et Biophysica Acta, 650 (1981) 21.

[74] H.Hauser, I.Pascher I. and S.Sundell, Conformation of phospholipids. Crystal structure of a lysophosphatidylcholine analogue, J. Mol. Biol. 137 (1980) 249.

[75] J.D.Roberts, and M.C.Caserio, Basic Principles of Organic Chemistry, second edition. W. A. Benjamin, Inc., Menlo Park, CA., 1977. ISBN 0-8053-8329-8.

Captions

Figure 1.

(a) DLS measurement of prepared vesicle dispersion. (b) Fluorescence of 1 μmol dm^{-3}; o-HO-BP at excitation = 295 nm (blue), m-HO-BP at excitation= 290 nm (black) and p-HO-BP at excitation = 288 nm (red), in the presence of 0.249 DOPC mmol dm^{-3} and 0.12 mol dm^{-3} of KI. All fluorescence values corrected for fluorescence in absence of BP and KI. (c) Modified Stern-Volmer plots for I$^-$ quenching of 1 μmol dm^{-3} p- (filled circle), m- (triangle) and o- (square) HO-BP in the presence of 0.249 mmol dm^{-3} DOPC vesicles in 0.1 mol dm^{-3} KCl with 0.001 mol dm^{-3} of phosphate.

Figure 2.

(a) Specific capacitance (C$_{sp}$)-potential (-E) plot of DOPC coated Hg electrode in 0.1 mol dm^{-3} KCl containing 0.001 mol dm^{-3} phosphate buffer as control (black) in the presence of 1.0 ⌈mol dm^{-3} o- (blue), m- (green) and p- (red) HO-BP; (b) Peak-1 specific capacitance (from (a)) versus BP concentration (c$_{BP}$) plots of o- (filled triangle), m- (filled inverted triangle) and p-(open square) HO-BP; (c) % peak-1 capacitance (relative to control from (a)) against accessible fraction from fluorescence measurements in 0.249 mmol dm^{-3} DOPC vesicle dispersion with 1.0 ⌈mol dm^{-3} of HO-BP; (d) Complex capacitance plane plots of DOPC coated Hg electrode in 0.1 mol dm^{-3} KCl containing 0.001 mol dm^{-3} phosphate buffer (black) in the presence of 1.0 ⌈mol dm^{-3} o- (blue), and p- (red) HO-BP.

Figure 3.

(a) Specific capacitance (C$_{sp}$)-potential (-E) plot of DOPC coated Hg electrode in 0.1 mol dm^{-3} KCl containing 0.001 mol dm^{-3} phosphate buffer as control (black) in the presence of 1.0 ⌈mol dm o- (blue), m- (green) and p- (red) Cl-BP; (b) Peak-1 specific capacitance (from (a)) versus concentration ((c$_{BP}$) plots of o- (filled triangle), m- (open triangle) and p-(filled square) Cl-BP; (c)

29

% peak-1 capacitance (relative to control from (a)) against accessible fraction from fluorescence measurements of DOPC vesicle dispersion with 1.0 ⌈mol dm^{-3} Cl-BP.

Figure 4.

(a) Complex capacitance plane plot of representative impedance data of DOPC coated Hg chip electrode in 0.1 mol dm^{-3} KCl with 0.001 mol dm^{-3} phosphate buffer (black) containing 1.0 μmol dm^{-3} of o- (blue) and p- (red) Cl-BP acquired using EIS at -0.4 V applied potential; (b) FIC$_{sp}$ from (a), versus BP concentration (c$_{BP}$) plot of o- (filled triangle), m- (open triangle) and p- (filled square) Cl-BP. Error bars are within the symbol size.

Figure 5.

Plot of BP substituent's Hammetts constants:- (a) σ$_t$ and, (b) σ$_m$ [35] against BPs accessible fraction to I$^-$ quenching on the DOPC bilayer with 1 μmol dm^{-3} BP in solution. Error bars within symbol size.

Figure 6.

Plot of FIC$_{sp}$ (closed triangle) of DOPC coated Hg against accessible fraction to I$^-$ quenching of substituted BP on the DOPC bilayer with 1 μmol dm^{-3} BP in solution. Horizontal red dashed line corresponds to FIC$_{sp}$ of pure DOPC. Error bars are within the symbol size.

Figure 1
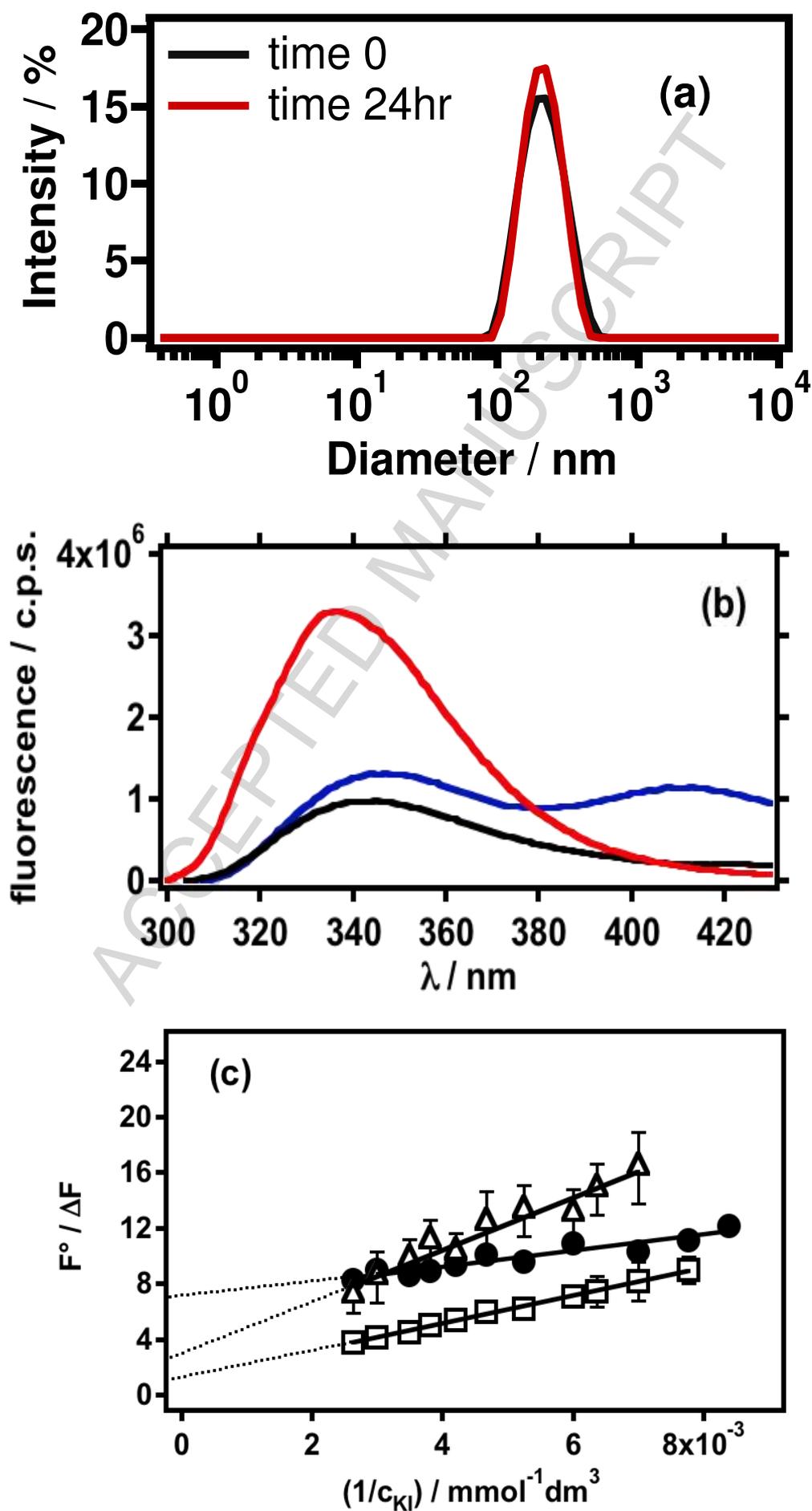
Figure 2
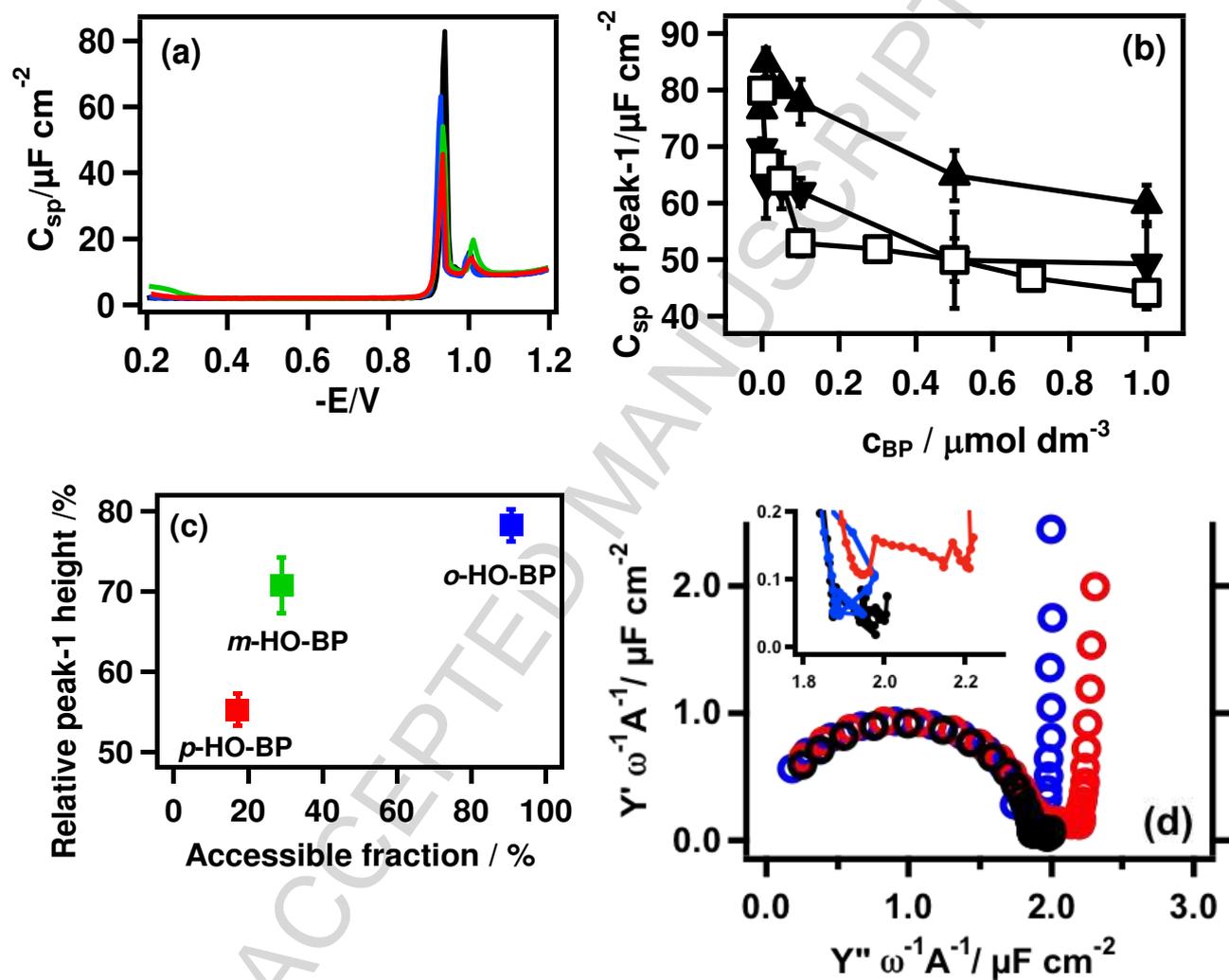
Figure 3
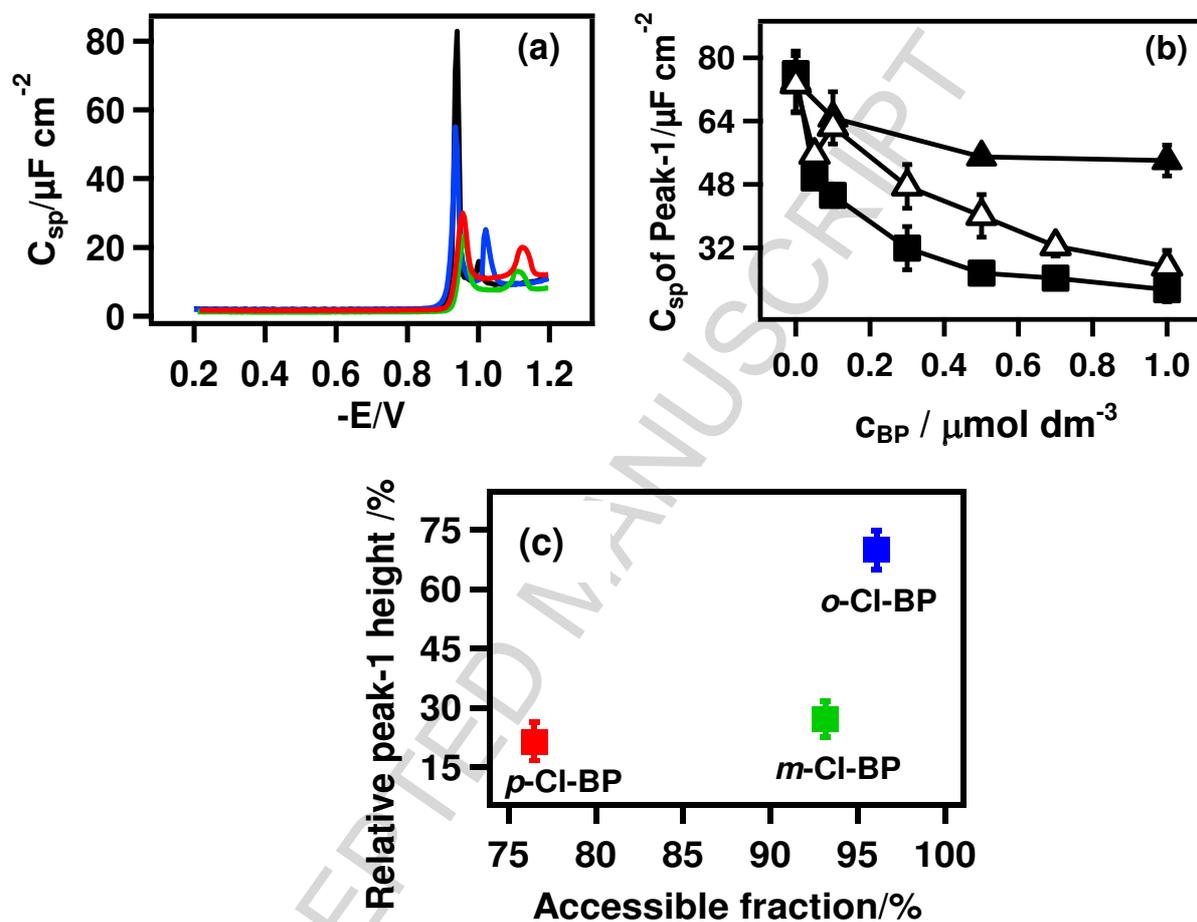
Figure 4
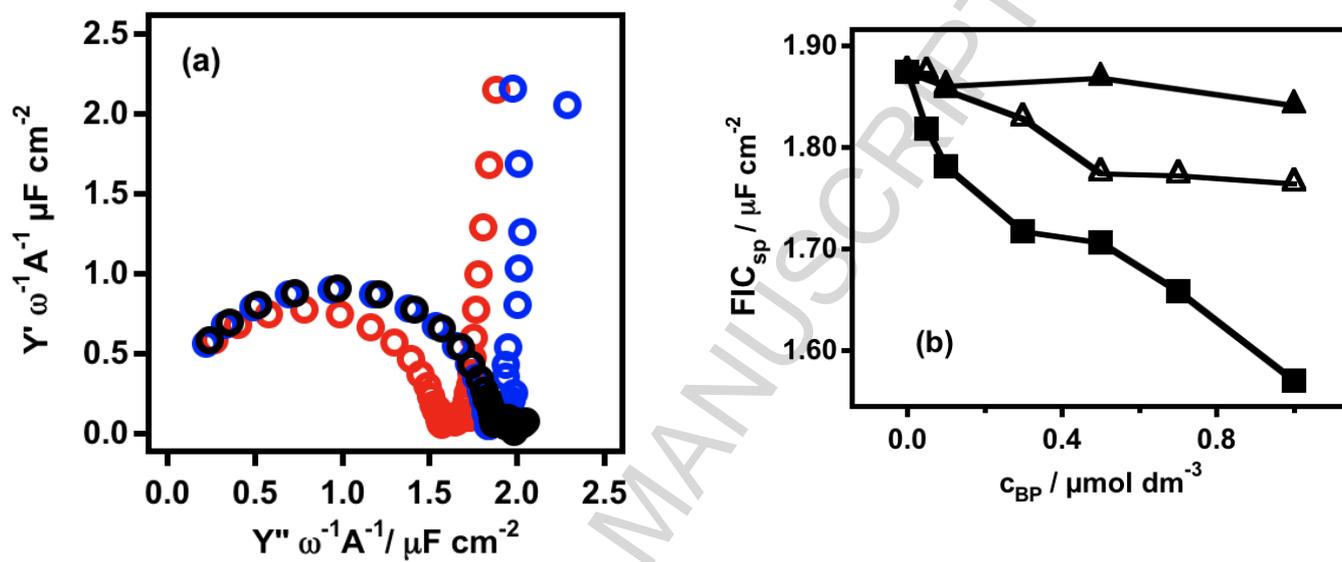
Figure 5
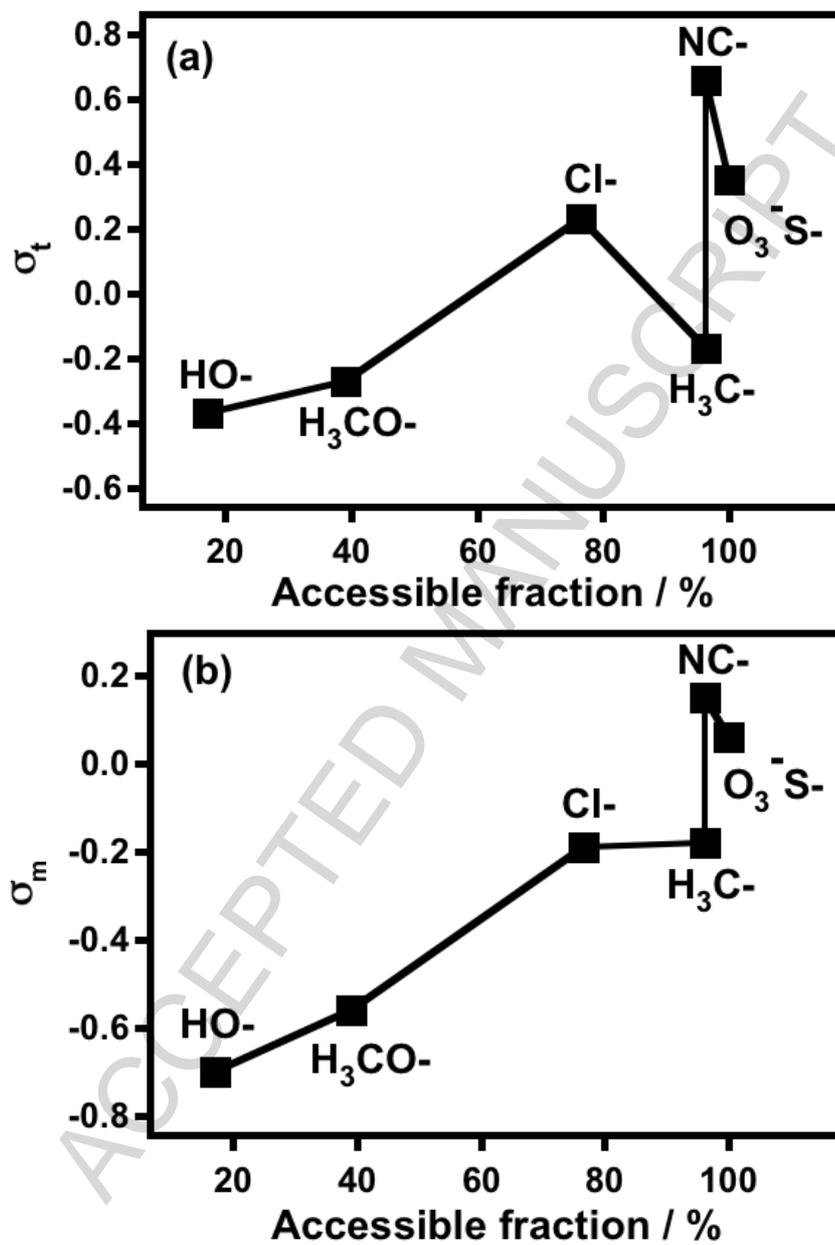
Figure 6
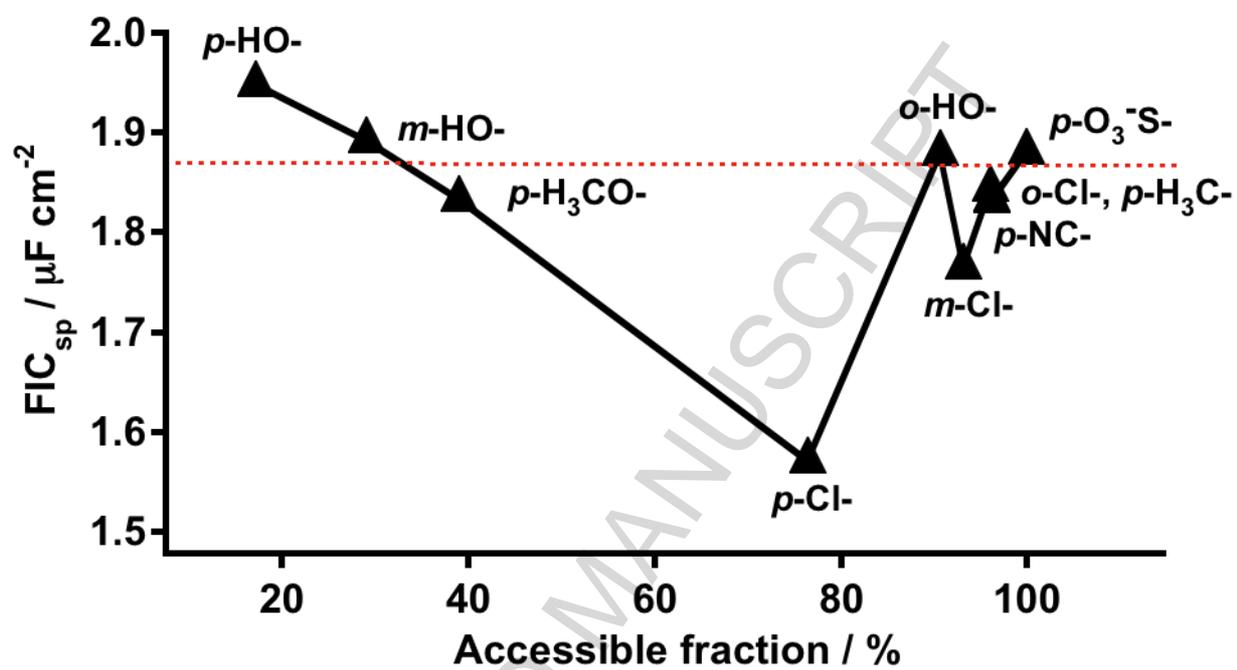
Table 1.

Log P [48], Hammetts constant ($\int_t$ and $\int_m$) [49] and torsional angle [16] ($\prod$) values.

Position	o		m		p					
Substitution	Cl-	HO-	Cl-	HO-	O_3^-S-	NC-	Cl-	HO-	H_3CO-	H_3C-
Log P	4.54	3.1	4.6	3.2	n/a	3.7	4.61	3.2	4.0	4.6
σ_t					0.35	0.66	0.23	-0.37	-0.27	-0.17
σ_m					0.06	0.15	-0.19	-0.7	-0.56	-0.18
φ	$45°\leq\varphi\geq60°$		$\varphi\sim45°$		$\varphi<45°$					

Table 2.

Binding energies of BP, Cl-BP, HO-BP and NC-BP molecules with CH_3-(CO)O-CH_3 (calculated with Schrodinger Jaguar software).

Complex A: structure	Binding energy, kcal mol^{-1}	Complex B: structure	Binding energy, kcal mol^{-1}
	1.55		1.5
	1.8		2.27
	1.31		1.03
	2.86		2.17
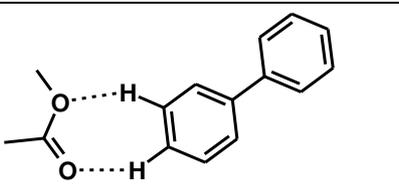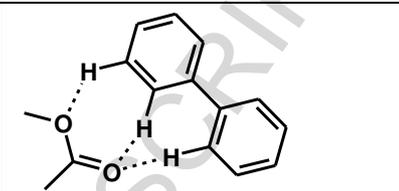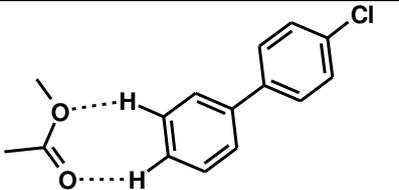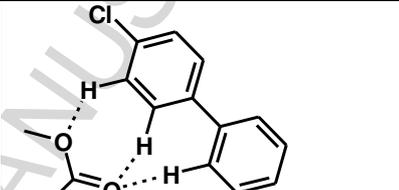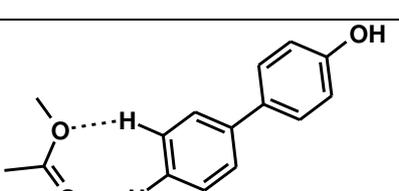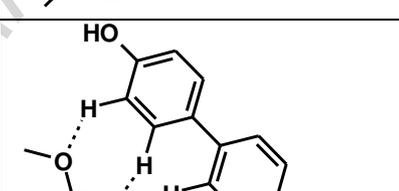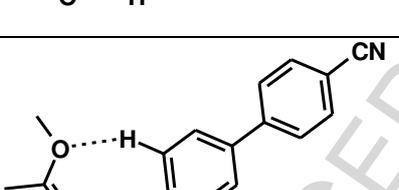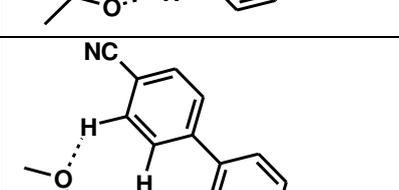
Table 3.

Binding energies of HO- (p-HO-BP) with CH_3-(CO)O-CH_3, Cl- (Cl-BP) with –PO_2^- of DOPC molecule and HOH with HOH; normalised per single bond (calculated with Schrodinger Jaguar software).

Structure	Binding energy, kcal mol^{-1}	Structure	Binding energy, kcal mol^{-1}
	7.43		2.18
	5.05		
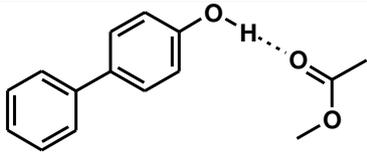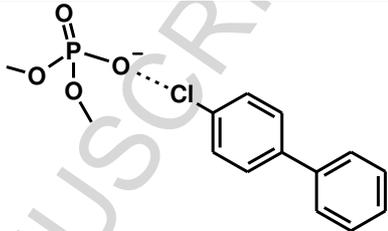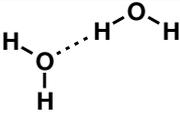
Graphical abstract
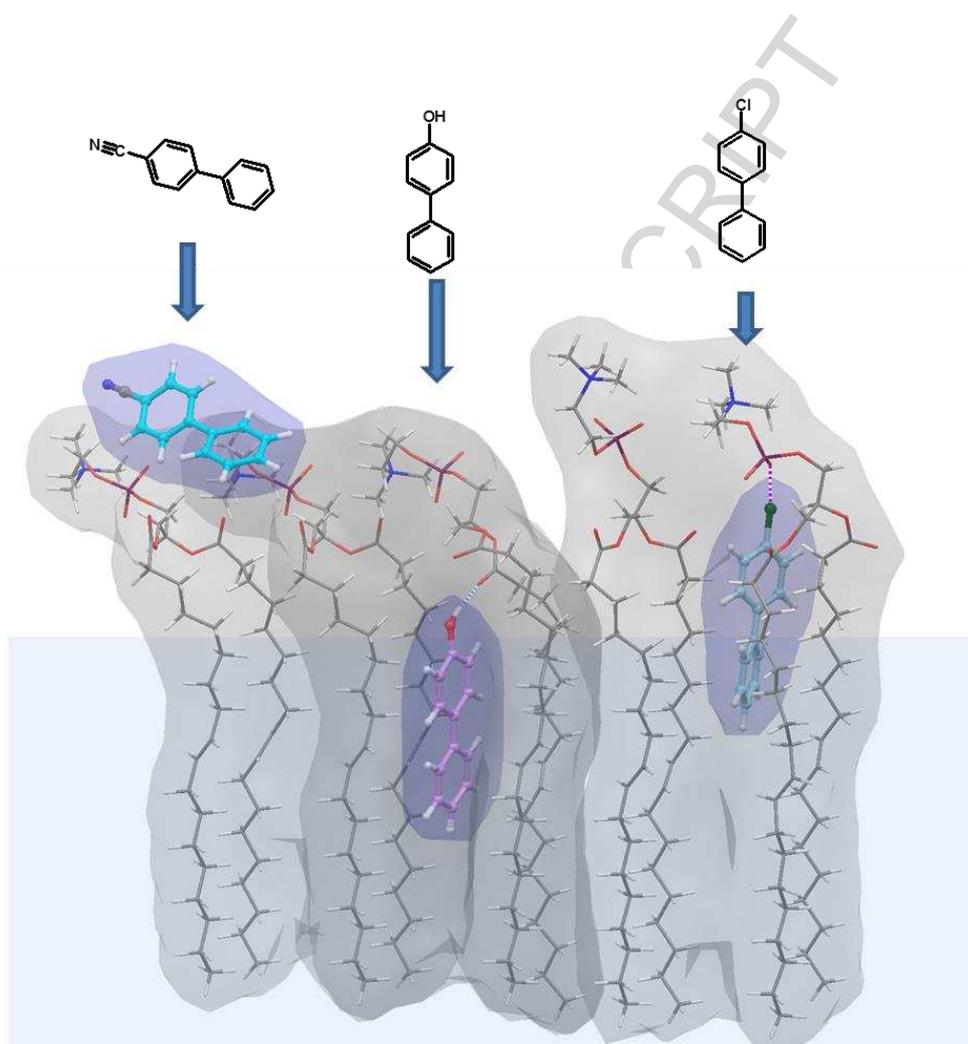
Highlights

Substituents modulate biphenyl penetration into lipid membranes

♦ Substituted biphenyls (BP) interact with DOPC membranes in the order p- > m- > o-

♦ Substituents modulate the penetration of BPs into DOPC membranes

♦ BP substituent position and ring polarizability influence BP/membrane interaction

♦ Monolayer/bilayer experiments give consistent results for BP/membrane interaction